ELSEVIER

Chemical Engineering Journal 135 (2008) 216–223

Chemical Engineering Journal

www.elsevier.com/locate/cej

Electrochemical promotion of bulk lattice-oxygen extraction for syngas generation over Ni-GDC anodes in direct-methane SOFCs

Ta-Jen Huang *, Meng-Chin Huang

Department of Chemical Engineering, National Tsing Hua University, Hsinchu 300, Taiwan, ROC

Received 25 January 2007; received in revised form 27 February 2007; accepted 7 March 2007

Abstract

Gadolinia-doped ceria (GDC), a mixed ionic-electronic conductor, was used to fabricate a Ni-GDC/GDC/Pt solid oxide fuel cell (SOFC). The Ni-GDC anode has a composition of Ni:GDC = 3:5 in weight. A new phenomenon of electrochemical promotion of lattice-oxygen extraction from GDC bulk is observed during direct methane oxidation, in the absence of anode-side gas-phase oxygen, to generate syngas at 800 °C. The extraction of markedly higher amount of oxygen than that of the measured current is promoted. This effect increases as the potential (the generated voltage) increases. Both rates of CO and CO_2 formations are linearly related to the measured current density but inversely linearly related to the voltage. The formation rate of CO depends on the rate of oxygen supply to the anode surface and its dependence is stronger than that of CO_2. As the oxygen-supply rate increases, both methane conversion and CO selectivity increase. Electrochemical promotion of bulk lattice-oxygen extraction enhances the syngas generation.

Keywords: Electrochemical promotion; Bulk lattice-oxygen extraction; Methane oxidation; Syngas generation; Solid oxide fuel cell; Gadolinia-doped ceria

1. Introduction

Non-faradaic electrochemical modification of catalytic activity (NEMCA) or electrochemical promotion effect has been studied extensively [1–8]. This effect is due to electrochemically controlled migration of ionic species from the solid electrolyte onto the gas-exposed electrode surface. Upon application of an external potential, the migration of ionic species onto the electrode surface causes a change in catalyst work function [9], which corresponds to a change in activation energy so as to affect the catalytic rate. In general, as the electrode potential increases, the oxidation rate increases for electrophobic behavior and decreases for electrophilic behavior [10].

The Faradaic efficiency (Λ) for electrochemical promotion is defined as:

$$\Lambda = \frac{\Delta r}{I/nF} \tag{1}$$

where Δr is the current- or potential-induced change in catalytic rate, I the applied current, n the charge of the electromigrating promoting species, and F is Faraday's constant [11]. It is pointed out that, with O^{2-}-conducting supports, only a fraction, i.e. $1/\Lambda$, of the oxygen species from the support will be found in the reaction products [12]. This fraction becomes significant only at elevated temperature, i.e. $T > 550$ °C, where Λ approaches unity and the phenomenon of electrochemical promotion disappears. In other words, when a positive (anodic) current I is applied, O^{2-} is supplied to the catalyst at a rate $I/2F$; this support-supplied lattice oxygen species can act as a reactant but the reaction rate due to this oxygen amount is limited by $I/2F$ [13]. It is also pointed out that two distinct types of oxygen present on supported metal surfaces, one promoting, the other highly active, are needed to complete the picture of the phenomenon for electrochemical promotion; consequently, the concept of the sacrificial promoter is essential for the interpretation of the effect of electrochemical promotion [12].

Methane decomposition over the Ni cermet anode is a major reaction in direct methane solid oxide fuel cell (SOFC) [14,15]. Since methane decomposition over the Ni cermet anodes generally causes carbon deposition (coking) [16], self de-coking can be an important reaction. Notably, "self de-coking" means the removal of the produced or deposited carbon-containing species by the oxygen species from the bulk lattice, when there is no oxygen in the gas phase [17]. In the case of direct-methane

* Corresponding author. Tel.: +886 3 5716260; fax: +886 3 5715408.
E-mail address: tjhuang@che.nthu.edu.tw (T.-J. Huang).

1385-8947/$ – see front matter © 2007 Elsevier B.V. All rights reserved.
doi:10.1016/j.cej.2007.03.015

SOFCs, self de-coking can be done by the oxygen species transported from the cathode three-phase boundary (TPB) to the anode surface via the electrolyte. Therefore, self de-coking in direct-methane SOFCs is accompanied by the generation of the electrical current. Notably, during methane decomposition and self de-coking, the formation of only CO but not CO_2 should help the selectivity of synthesis gas (syngas), i.e. $CO + H_2$, for direct-methane SOFCs to generate syngas.

In this work, a phenomenon of electrochemical promotion of lattice-oxygen extraction from anode-side bulk of gadolinia-doped ceria (GDC) is observed during methane oxidation over Ni-GDC anodes in SOFCs operating at 800 °C without oxygen in the anode-side gas phase. This work is the first report, as far as the authors know, on electrochemical promotion of bulk lattice-oxygen extraction from mixed ionic-electronic conducting materials, such as GDC [18]. This electrochemical promotion effect results in the extraction of markedly higher amount of oxygen, for anodic oxidation, than that of the measured current. This effect is induced by the migration of the oxygen species from the cathode TPB to the anode TPB via the electrolyte. The lattice-oxygen species from the anode-side bulk are highly active and both rates of CO and CO_2 formations are substantially enhanced. This is a case that the concept of the sacrificial promoter is not applicable. Thus, there should be a difference in electrochemical promotion between the case with oxygen in the anode-side gas phase and the case without it. It is also found that the electrochemical promotion effect on CO formation can be much higher than that on CO_2 formation. This is beneficial for syngas generation in direct-methane SOFC.

2. Experimental

2.1. Preparation of gadolinia-doped ceria

Gadolinia-doped ceria (GDC) was prepared by a co-precipitation method. The details of the method have been reported elsewhere [19]. The calcinations of the GDC powders were carried out by heating in air at a rate of 10 °C/min to 300 °C and held for 2 h, and then to 700 °C and held for 4 h, and then slowly cooled down to room temperature.

2.2. Preparation of Ni-GDC powder

The Ni-GDC powder for the anode is prepared by impregnating the above-prepared GDC powders (325–270 mesh, i.e. 44–53 μm diameter) with an aqueous solution of nickel nitrate (98% purity) in a ratio to make 60 wt.% Ni with respect to GDC. The mixture is heated with stirring to remove excess water and then place in a vacuum oven to dry overnight. The dried Ni-GDC powder is heated to 900 °C and then cooled down to room temperature. After milling, the Ni-GDC powder with Ni:GDC = 3:5 in weight was obtained.

2.3. Construction of SOFC unit cell

The GDC tape (150 μm thickness, Institute of Nuclear Energy Research, Taiwan, ROC) was employed to make an electrolyte-supported cell. A disk of 1.25 cm diameter was cut from the tape. One side of the disk was coated with the Ni-GDC paste, which was made of the above Ni-GDC powder, coin oil, polyvinyl butyral, and ethanol. The other side of the disk was screen-printed with a thin layer of Pt paste (C3605P, Heraeus) to make the cathode layer.

The coating of the Ni-GDC paste to make the anode layer was carried out by spinning coating with 2000 rpm for designated times. Then, the both side-coated unit cell was heated in an oven, with a heating rate of 5 °C/min, to 300 °C, held for 2 h, then to 500 °C, held for 2 h, and then to 1400 °C, held for 2 h. The thus-prepared unit cell has an anode area of 1 cm^2, an anode thickness of about 45 μm, an electrolyte thickness of 150 μm, a cathode area of 1 cm^2, and a cathode thickness of about 5 μm.

Both sides of the completed unit cell were closely connected with gold mesh wires (100 mesh) for current collection, and then with Pt wires to the current and voltage measurement units. The ceramic paste was used to seal the unit cell in a quartz tube with a heat treatment of 400 °C for 1.5 h so as to complete the preparation of the test unit. The anode side of the unit cell is sealed in the quartz tube and the cathode side is exposed to stagnant air.

2.4. Activity test of direct-methane oxidation

An external circuit resistance of 1 Ω, which is the lowest adjustable resistance of the load circuit in this work, was employed for some operations. For others, the external circuit resistance is varied, as described in the results. The test temperature is 800 °C throughout this work. The methane feed was always 10% CH_4 in argon. The flow rate was always 100 ml/min passing the anode side.

The test started with anode reduction at 400 °C with 10% H_2 for 2 h. Then, argon flow was passed for 2 h to purge the system. The test unit was then heated in argon to 800 °C at a rate of 5 °C/min. Then, 10% H_2 was introduced for 30 min and argon flow was followed until the measured electrical current became zero. Test of direct-methane oxidation was then carried out with introducing CH_4 flow for a designated time, followed by argon flow till both CO and CO_2 formations as well as the measured electrical current became zero. Then, 20% O_2 was introduced till CO and CO_2 formations became zero. Finally, argon flow was passed for 30 min to purge the system.

A new test started with the above-described introduction of 10% H_2 for 30 min at 800 °C and followed with argon flow until the measured electrical current became zero. However, if this H_2 test result showed a deactivation of the used unit cell, a fresh unit cell would be used and the new test started with the above-described anode reduction at 400 °C.

Through out the test, electrical current, voltage, and outlet gas compositions were always measured. The compositions of CO and CO_2 were measured by CO-NDIR and CO_2-NDIR (non-dispersive infrared analyzer, Beckman 880), respectively. Other gas compositions were measured by two gas chromatographs (China Chromatography 8900) in series.

3. Results and discussion

3.1. Electrochemical promotion of bulk lattice-oxygen extraction

Preliminary results indicate that a gas mixture of H_2 and CO with a ratio close to that of syngas for methanol, i.e. $H_2/CO = 2$, can be produced via direct methane oxidation over Ni-GDC anodes. For partial oxidation of methane to produce syngas, the oxygen species are considered to come from the cathode-side gas phase via the electrolyte. However, every case of Fig. 1 reveals that the equivalent current is much higher than that of the measured current. Notably, the equivalent current as shown in Fig. 1 indicates the current which would be produced if the O species for the formation of CO_x, i.e. CO and CO_2, at the anode three-phase boundary (TPB) come from the cathode TPB; the equivalent current is thus calculated by [(CO formation amount) + (CO_2 formation amount) × 2]/0.31088]. Notably, also, the oxygen-transfer rate and the current density, the right and left ordinate of Fig. 1, is related by 0.31088 μmol O^{2-}/cm^2 min to 1 mA/cm^2. In other words, the indicated equivalent current shows the total amount of CO_x formation. Notably, also, a measured current can occur only with the oxygen species transported from the cathode TPB to the anode TPB. Therefore, the oxygen amount needed for CO_x formation is much higher than that supplied from the cathode-side gas phase. This means that additional amount of lattice oxygen is extracted from the anode side. In other words, the oxygen species for partial oxidation of methane can come from either the cathode-side gas phase or the anode-side lattice. As the Ni-GDC anode is reduced at 800 °C in this work, the additionally extracted oxygen species should come from the GDC bulk, noting that NiO can be completely reduced to Ni at 400 °C [20] and the surface lattice oxygen of GDC can be completely removed at about 530 °C [21]. This shows a phenomenon of electrochemically promoted lattice-oxygen extraction from the anode-side GDC bulk. This indicates that the amount of the support-supplied lattice oxygen for the anodic reaction is not limited by $I/2F$ and thus reveals a new type of electrochemical promotion. This is reported here for the first time, as far as the authors know, on the mixed ionic-electronic conductor, such as GDC used in this work.

The amount of the additionally extracted oxygen is indicated as zone I in Fig. 1. Notably, zone I denotes the area between the curves of equivalent current and measured current and extends

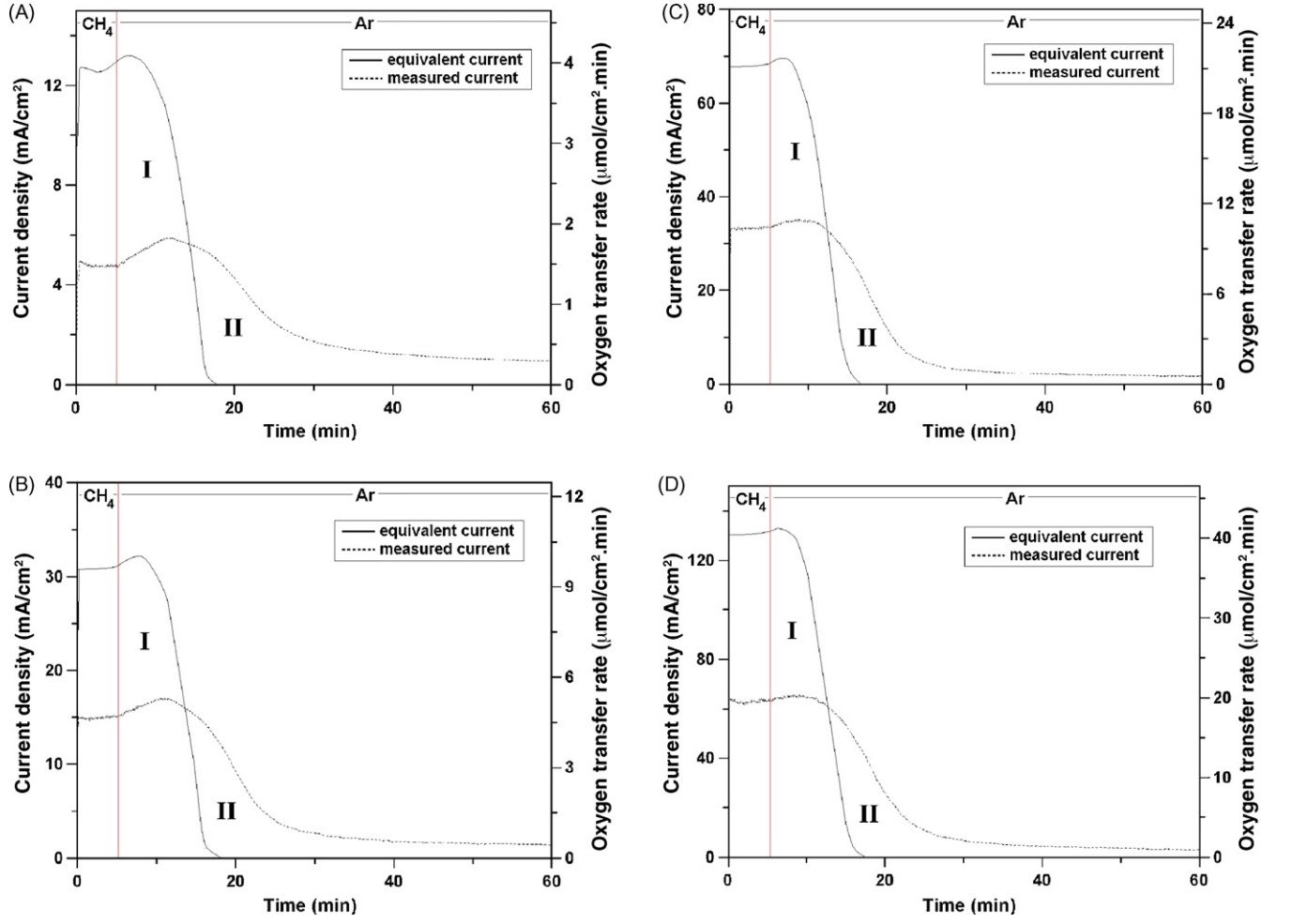

Fig. 1. Profiles of current densities vs. time (5 min CH_4 flow). A–D as in Table 1. Zone I denotes the area between the curves of equivalent current and measured current and extends from time zero until these two curves meet. Zone II denotes the area under the curve of measured current and to the right of the curve of equivalent current.

Table 1
Relations of voltage and current density with circuit resistance as well as total amounts of O species transported and extracted during 5 min CH_4 flow

Case Case	External circuit) resistance (Ω)	Voltage (V)	Current density[a] (mA/cm^2)	O species transported[b] (μmol/cm^2)	Lattice O extracted[c] (μmol/cm^2)
A	12,000	0.51	4.62	7.18	12.86
B	31	0.43	14.85	23.08	25.43
C	8.4	0.34.	32.97	51.09	56.65
D	1	0.17	62.6	97.3	107.8

[a] Average value of the measured current density during 5 min CH_4 flow. The area is in terms of the anode area. Current density = current/(anode area).
[b] The amount of oxygen species transported from cathode TPB for the generation of the measured current. This equals (total measured current density during 5 min methane flow) × 0.31088.
[c] The amount of lattice oxygen species additionally extracted from anode-side bulk. This equals (total CO formation amount in 5 min CH_4 flow) + (total CO_2 formation amount in 5 min CH_4 flow) × 2 − (O species transported) + (O species for H_2O formation).

from time zero until these two curves meet. The oxygen amount for CO_x production as indicated by the equivalent current is also represented by the oxygen-transfer rate. The CO_x equivalent current is calculated with the total amount of the O species in forming CO and CO_2, with each O species carrying two electrons. The equivalent current as shown in Fig. 1 is equivalent to the formation rate of CO_x only; it should be equivalent to the total rate of formation of all the oxidation products. Therefore, the formation rate of other detectable oxidation products, only H_2O in this work, is included to calculate the total amount of lattice oxygen extracted for oxidation, such as those shown in Table 1. Nevertheless, the amount of H_2O formed from CH_4 reactions was quite small during all the experiments of this work; consequently, although H_2O was measured by GC whose accuracy is less than that of CO_x measured by NDIR, the total amount of lattice-oxygen extraction can be calculated with sufficient accuracy.

Fig. 1 reveals also a region, designated as zone II, for the generation of electrical current in the absence of any fuel, either in the gas phase or over the anode surface, the latter being the deposited carbon species from methane decomposition. Notably, zone II denotes the area under the curve of measured current and to the right of the curve of equivalent current. A combination of Fig. 1 and Fig. 2 reveals the evidence for the absence of any fuel in relation to the occurrence of zone II. Fig. 2 shows that CO_x formations become zero well before 20 min. Separate GC measurements indicate that H_2O formation is quite small and becomes zero well before CO_x does. Notably, also, the profile of the equivalent current indicates the amount of CO_x formation. Therefore, the electrical current designated by zone II is indeed a current generated in the absence of any fuel and can be termed a "fuel-free current" [22]. The occurrence of the fuel-free current is considered to be due to the electrochemically promoted extraction of lattice oxygen from the anode-side bulk during the oxidation of the fuel. Notably, also, the value of the possible electrical current accompanying oxygen pumping in tests of pure Ar flow over the anode was under the detection limit of this work, i.e. 0.01 mA, and is thus considered to be zero.

In this work, the "fuel" means both methane and the deposited carbon species from methane decomposition. These carbon species are usually considered to be surface CH_x (x = 0–3) species, which are intermediates of CH_4 decomposition over Ni [23]. Since H_2O formation becomes zero well before CO_x does, the deposited carbon species can be the C species, which may cause coking to deactivate the anode. Separate tests indicate that anode deactivation did not occur with 5 min methane flow but may occur with longer methane flow; thus, methane flow of only 5 min is employed for the measurements in this work to prevent the effect of anode deactivation.

The occurrence of the fuel-free current is considered to be due to the deficiency of bulk lattice-oxygen concentration on the anode side after oxidations of methane and the deposited carbon species, which extract additional amount of the lattice oxygen from the anode-side bulk without replenishment from the cathode TPB. Consequently, a deficiency of bulk lattice-

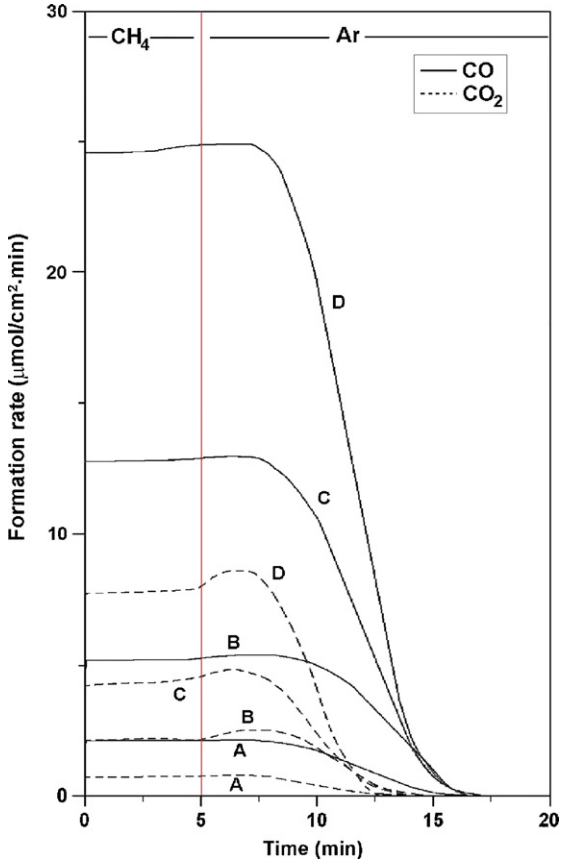

Fig. 2. Profiles of CO and CO_2 formation rates vs. time (5 min CH_4 flow). A–D as in Table 1.

oxygen concentration on the anode side is build up during the oxidation of the fuel and thus, afterwards, the oxygen species migrate from the cathode TPB to the anode side to replenish the bulk lattice-oxygen concentration on the anode side to its initial state, which generates an electrical current. Therefore, the occurrence of the fuel-free current is a consequence of the electrochemically promoted extraction of bulk lattice oxygen from the anode side.

3.2. Effect of current density

Table 1 indicates that the voltage decreases and the current density increases as the external circuit resistance decreases. Notably, when the external circuit resistance decreases, the electron flowing rate (current) increases in the external circuit; this results in an increase of the current density, that is, an increase of the transfer rate of the oxygen ion, the electron carrier, in the GDC bulk lattice. In other words, higher current density means higher mobility of the lattice O species. Fig. 1(A)–(D) presents the results of the variations of current density with time under different circuit resistance. The phenomenon of electrochemical promotion of bulk lattice-oxygen extraction, indicated by zone I, and that of fuel-free current, indicated by zone II, occurs in all cases. Notably, the profile of the equivalent current indicates the CO_x formation. From case A to case D, with increasing current density, the lattice O species which can be additionally extracted from the anode-side bulk increases, as also shown in Table 1. Consequently, the profile of the fuel-free current, the zone II profile, can become zero faster, indicating a higher mobility of the lattice O species for the replenishment of the anode-side lattice oxygen.

Table 1 shows that, as the current density increases, the amount of bulk lattice-oxygen extraction increases. Additionally, the electron charge per O species supplied for anodic oxidation is close to or smaller than one, indicating possible occurrence of the O^- ion. Notably, the electron charge per O species is calculated by dividing the total number of electrons of the electrical current with the total amount of oxygen supplied to the anode surface. The total amount of the oxygen species is the sum of those transported form cathode TPB and those additionally extracted from the anode-side GDC bulk. Notably, also, the oxygen species for generating the measured current is from the cathode-side gas phase via dissociation and charge transfer, that is, $O_2 \leftrightarrows 2O$ and then $O + 2e^- \leftrightarrows O^{2-}$. The O^{2-} ion is generally considered to be the form of the oxygen ion, which diffuses in the bulk lattice. However, at the electrode TPB, the following scheme of oxygen reduction is generally adopted: $O_2 \leftrightarrows {O_2}^- \leftrightarrows {O_2}^{2-} \leftrightarrows 2O^- \leftrightarrows 2O^{2-}$, where the O^{2-} species is subsequently incorporated into the oxygen vacancy [24]. Thus, when the O^{2-} ion is transported to the anode side, it may donate an electron to the bulk lattice oxygen to form the O^- ion. This electron transfer in the GDC bulk is possible since GDC is a mixed ionic-electronic conductor. This is considered to increase the mobility of the lattice-oxygen species. Consequently, additional amount of the lattice-oxygen species in the anode-side bulk can be extracted and transported to the anode surface for CO_x formations. Table 1 reveals that the effect of the electrochemical promotion of bulk lattice-oxygen extraction is additional to that of electrocatalysis associated with the oxygen species transported from the cathode TPB.

Table 2
Amounts of total CO_x formation during CH_4 plus argon flow and O_2 de-coking as well as O_2 de-coking time

Case[a]	CO_x formation[b] (μmol/cm^2)		O_2 de-coking time[c] (min)
	CH_4 plus Ar flow[d]	O_2 de-coking[e]	
A	37.1	5.43	629
B	81.6	2.98	356
C	142.7	0.77	57
D	301.2	0.21	16

[a] A–D as in Table 1.
[b] CO_x means both CO and CO_2. The area is in terms of the anode area.
[c] The time for O_2 de-coking till zero CO_2 formation.
[d] From the start of methane flow into argon flow until both CO and CO_2 formations became zero. The methane flow was 5 min.
[e] Removal of the remaining coke with 100 ml/min of 20% O_2 in argon at 800 °C. Only CO_2 was detected.

Table 2 reveals that, with increasing current density from case A to case D, the amount of total CO_x formations during methane plus argon flow increases but that during O_2 de-coking decreases; moreover, the O_2 de-coking time also decreases. This indicates that the SOFC ability to utilize the deposited carbon species for the co-generation of electrical current and syngas increases with increasing current density. Notably, longer O_2 de-coking time means a more severe coking problem, that is, the formation of higher amount of non-removable coke over the anode to deactivate it. Therefore, higher current density can reduce the coking problem.

3.3. Promotion of syngas generation

Fig. 2 shows that the formation rate of CO is much higher than that of CO_2 for every case and there is a period of the formation of only CO but not CO_2. This is beneficial for syngas generation. From case A to case D, with the increase of the total rate of oxygen supply for the anodic oxidation, both CO and CO_2 formation rates increase. Nevertheless, the extent of the increase of the CO formation rate is higher than that of CO_2 and thus the CO selectivity increases. These are also revealed in Table 3. Therefore, higher oxygen-supply rate is beneficial for the generation of syngas. In other words, the electrochemically promoted extraction of bulk lattice oxygen is beneficial for syngas generation.

Table 3
Total amounts of CO and CO_2 formations and CO selectivity during 5 min CH_4 flow

Case[a]	CO (μmol/cm^2)	CO_2 (μmol/cm^2)	CO selectivity[b]
A	8.43	5.59	0.601
B	25.99	10.79	0.707
C	63.28	21.47	0.747
D	124.26	39.66	0.758

[a] A–D as in Table 1.
[b] CO selectivity = amount of CO/(amount of CO + amount of CO_2).

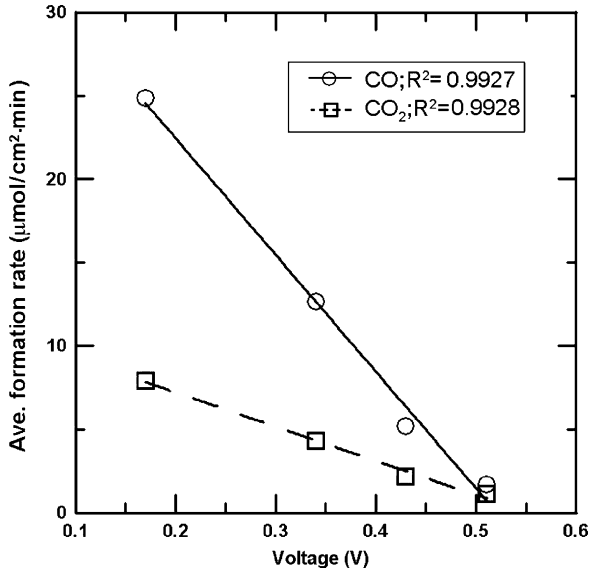

Fig. 3. Linear regression variations of the rates of CO and CO_2 formations with voltage.

Fig. 3 shows that the average formation rates of both CO and CO_2 are inversely linearly related to the voltage. Since both CO and CO_2 formation rates are enhanced by the electrochemically promoted extraction of bulk lattice oxygen, their rate behaviors may be explained by the rule of electrochemical promotion [8]. This is indeed the case as Fig. 3 shows the well-known relationship that the effect of electrochemical promotion increases with decreasing potential (electrophilic behavior).

Fig. 4 shows that the average formation rates of both CO and CO_2 are linearly related to current density. Nevertheless, the effect of electrochemical promotion on CO can be much higher than that on CO_2 at higher oxygen-supply rate, as a combination of Table 1 and Table 3 shows. Moreover, Table 4 reveals that the

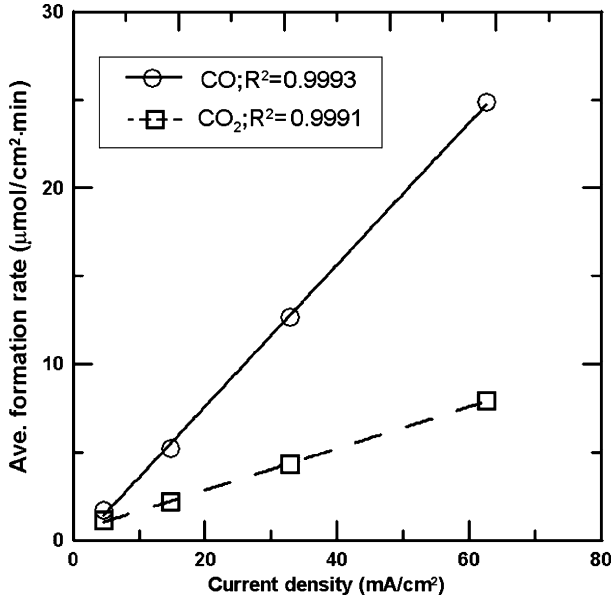

Fig. 4. Linear regression variations of the rates of CO and CO_2 formations with current densities.

Table 4
Variations of CO and CO_2 formed per oxygen supplied[a] to the anode surface during 5 min CH_4 flow

Case[b]	CO/O	CO_2/O
A	0.421	0.279
B	0.536	0.222
C	0.587	0.199
D	0.606	0.193

[a] O species transported plus lattice O extracted.
[b] A–D as in Table 1.

Table 5
Results of regression analysis ($R = ax^n$) of average formation rate[a] (R) of CO and CO_2 vs. average oxygen-supply rate[b] (x)

Reaction	a	n
CO formation	0.4483	1.0819
CO_2 formation	0.2784	0.9002

[a] Calculated by dividing the total formation rate of CO and CO_2, respectively, during 5 min CH_4 flow by 5 min.
[b] Calculated by dividing the total oxygen-supply rate, i.e. O species transported plus lattice O extracted, during 5 min CH_4 flow by 5 min.

formation rate of CO per O species supplied to the anode surface increases but that of CO_2 decreases with increasing oxygen-supply rate, from case A to D. This promotes syngas generation.

The average formation rate (R) of CO and CO_2 can be related to the average supply rate (x) of the oxygen species supplied to the anode surface:

$$R = ax^n \quad (2)$$

Table 5 presents the constants a and n from a regression analysis, shown in Fig. 5. It is seen that the rate dependence of CO formation on the oxygen-supply rate is higher than that of CO_2 formation.

The above results indicate that higher CO and CO_2 formation rates, i.e. higher methane conversion, are accompanied

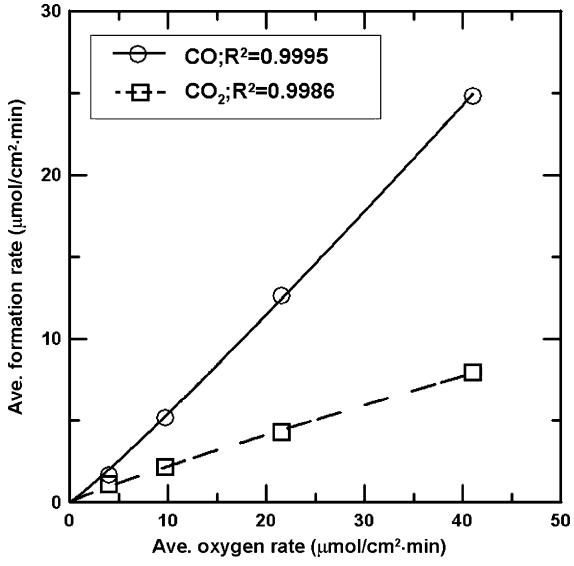

Fig. 5. Regression analysis ($R = ax^n$) of average formation rate (R) of CO and CO_2 vs. average oxygen-supply rate (x).

by higher CO selectivity. Moreover, the electrochemically promoted extraction of bulk lattice oxygen results in higher CO selectivity. These are beneficial for syngas generation. With methane decomposition in the absence of gaseous oxygen, the formations of CO and CO_2 occur by oxidation with the oxygen species migrating from the support lattice to the metal surface via the metal–support interface [25]. Thus, electrochemical promotion of bulk lattice-oxygen extraction increases the supply rate of the oxygen species to the anode surface; consequently, the rates of CO and CO_2 formations are promoted. This promotion of the CO and CO_2 formation rates is partly due to the effect of electrocatalysis by current flow and partly due to that of electrochemical promotion of bulk lattice-oxygen extraction. Table 1 reveals that the latter effect is higher than the former one. Additionally, with increased current density, the absolute amount of the electrochemically promoted oxygen extraction increases, shown in Table 1. Therefore, electrochemical promotion of bulk lattice-oxygen extraction enhances the syngas generation in both productivity and selectivity.

Since the CO formation rate depends on the oxygen-supply rate to a higher extent than the CO_2 formation rate, revealed in Table 5, the increased oxygen-supply rate by either the effect of electrocatalysis of current flow or that of electrochemical promotion of bulk lattice-oxygen extraction should result in a higher rate of CO formation than that of CO_2 formation per oxygen species supplied to the anode surface. This is in agreement with the results of Table 4.

Table 4 shows that higher oxygen-supply rate is beneficial to the formation of CO, but detrimental to that of CO_2. This is attributable to that CO_2 formation requires two O species in the neighborhood of the C species. If there is only one O species in the neighborhood of the C species during the reaction time, only CO can be formed. Consequently, if the oxygen-supply rate increases, which means an increased mobility of the O species, the probability of the existence of two O species in the neighborhood of the C species during its reaction time should decrease; this probability decreases with shorter reaction time. Notably, the oxygen-supply rate indicates the migration speed of the O species through the anode surface; a higher migration speed of the O species means a shorter reaction time for the oxidation of the C species. Consequently, faster migration of the O species favors CO formation. This is in agreement with the result of Huang and Wang [26] that the CO and CO_2 formation rates can be controlled by the mobility of the bulk lattice oxygen. It can thus be concluded that SOFC operation at higher oxygen-supply rate favors syngas generation. Moreover, this higher CO selectivity associated with higher rate of oxygen supplied from the bulk lattice is a phenomenon quite different from that associated with higher rate of oxygen supplied from the anode-side gas phase, the latter lowering the CO selectivity.

4. Conclusions

(1) A new phenomenon of electrochemical promotion of lattice-oxygen extraction from the bulk phase of GDC, a mixed ionic-electronic conductor, is observed during direct methane oxidation, in the absence of anode-side gas-phase oxygen, to generate syngas at 800 °C.
(2) The extraction of markedly higher amount of oxygen than that of the measured current is promoted.
(3) The effect of electrochemical promotion of bulk lattice-oxygen extraction increases as the potential (the generated voltage) increases.
(4) Both rates of CO and CO_2 formations are inversely linearly related to the voltage.
(5) Both rates of CO and CO_2 formations are linearly related to the current density.
(6) The formation rate of CO depends on the rate of oxygen supply to the anode surface and its dependence is stronger than that of CO_2.
(7) As the oxygen-supply rate increases, both methane conversion and CO selectivity increase.
(8) Electrochemical promotion of bulk lattice-oxygen extraction enhances the syngas generation.

References

[1] C.G. Vayenas, S. Bebelis, S. Ladas, Dependence of catalytic rates on catalyst work function, Nature 343 (1990) 625–627.
[2] C.G. Vayenas, S. Bebelis, I.V. Yentekakis, H.G. Lintz, Non-faradaic electrochemical modification of catalytic activity: a status report, Catal. Today 11 (1992) 303–442.
[3] A. Kaloyannis, C.G. Vayenas, Non-faradaic electrochemical modification of catalytic activity – 12. Propylene oxidation on Pt, J. Catal. 182 (1999) 37–47.
[4] J. Nicole, D. Tsiplakides, C. Pliangos, X.E. Verykios, Ch. Comninellis, C.G. Vayenas, Electrochemical promotion and metal–support interactions, J. Catal. 204 (2001) 23–34.
[5] T. Tagawa, K. Kuroyanagi, S. Goto, S. Assabumrungrat, P. Praserthdam, Selective oxidation of methane in an SOFC-type reactor: effect of applied potential, Chem. Eng. J. 93 (2003) 3–9.
[6] C. Kokkofitis, G. Karagiannakis, S. Zisekas, M. Stoukides, Catalytic study and electrochemical promotion of propane oxidation on Pt/YSZ, J. Catal. 234 (2005) 476–487.
[7] D. Tsiplakides, S. Balomenou, A. Katsaounis, D. Archonta, C. Koutsodontis, C.G. Vayenas, Electrochemical promotion of catalysis: mechanistic investigations and monolithic electropromoted reactors, Catal. Today 100 (2005) 133–144.
[8] S. Brosda, C.G. Vayenas, J. Wei, Rules of chemical promotion, Appl. Catal. B: Environ. 68 (2006) 109–124.
[9] D. Tsiplakides, C.G. Vayenas, Temperature programmed desorption of oxygen from Ag films interfaced with Y_2O_3-doped ZrO_2, J. Catal. 185 (1999) 237–251.
[10] S. Bebelis, M. Makri, A. Buekenhoudt, J. Luyten, S. Brosda, P. Petrolekas, C. Pliangos, C.G. Vayenas, Electrochemical activation of catalytic reactions using anionic, cationic and mixed conductors, Solid State Ionics 129 (2000) 33–46.
[11] C.G. Vayenas, Thermodynamic analysis of the electrochemical promotion of catalysis, Solid State Ionics 168 (2004) 321–326.
[12] C.G. Vayenas, S. Brosda, C. Pliangos, The double-layer approach to promotion, electrocatalysis, electrochemical promotion, and metal–support interactions, J. Catal. 216 (2003) 487–504.
[13] A. Katsaounis, Z. Nikopoulou, X.E. Verykios, C.G. Vayenas, Comparative isotope-aided investigation of electrochemical promotion and metal–support interactions. 2. CO oxidation by $^{18}O_2$ on electropromoted Pt films deposited on YSZ and on nanodispersed Pt/YSZ catalysts, J. Catal. 226 (2004) 197–209.
[14] J.B. Wang, J.C. Jang, T.J. Huang, Study of Ni-samaria-doped ceria anode for direct oxidation of methane in solid oxide fuel cells, J. Power Sources 122 (2003) 122–131.

[15] Y. Lin, Z. Zhan, J. Liu, S.A. Barnett, Direct operation of solid oxide fuel cells with methane fuel, Solid State Ionics 176 (2005) 1827–1835.
[16] C. Mallon, K. Kendall, Sensitivity of nickel cermet anodes to reduction conditions, J. Power Sources 145 (2005) 154–160.
[17] J.B. Wang, Y.S. Wu, T.J. Huang, Effects of carbon deposition and de-coking treatments on the activation of CH_4 and CO_2 in CO_2 reforming of CH_4 over Ni/yttria-doped ceria catalysts, Appl. Catal. A: Gen. 272 (2004) 289–298.
[18] W.Z. Zhu, S.C. Deevi, A review on the status of anode materials for solid oxide fuel cells, Mater. Sci. Eng. A362 (2003) 228–239.
[19] T.J. Huang, T.C. Yu, Effect of steam and carbon dioxide pretreatment on methane decomposition and carbon gasification over doped-ceria supported nickel catalyst, Catal. Lett. 102 (2005) 175–181.
[20] J.B. Wang, S.Z. Hsiao, T.J. Huang, Study of carbon dioxide reforming of methane over Ni/yttria-doped ceria and effect of thermal treatments of support on the activity behaviors, Appl. Catal. A: Gen. 246 (2003) 197–211.
[21] T.J. Huang, H.J. Lin, T.C. Yu, A comparison of oxygen-vacancy effect on activity behaviors of carbon dioxide and steam reforming of methane over supported nickel catalysts, Catal. Lett. 105 (2005) 239–247.
[22] T.J. Huang, M.C. Huang, A new phenomenon of a fuel-free current during intermittent fuel flow over Ni-YSZ anode in direct methane SOFCs, J. Power Sources 168 (2007) 229–235.
[23] Q.Y. Yang, K.J. Maynard, A.D. Johnson, S.T. Ceyer, The structure and chemistry of CH_3 and CH radicals adsorbed on Ni(1 1 1), J. Chem. Phys. 102 (1995) 7734–7749.
[24] J. Zhu, J.G. van Ommen, H.J.M. Bouwmeester, L. Lefferts, Activation of O_2 and CH_4 on yttrium-stabilized zirconia for the partial oxidation of methane to synthesis gas, J. Catal. 233 (2005) 434–441.
[25] T.J. Huang, S.Y. Jhao, Ni-Cu/samaria-doped ceria catalysts for steam reforming of methane in the presence of carbon dioxide, Appl. Catal. A: Gen. 302 (2006) 325–332.
[26] T.J. Huang, C.H. Wang, Methane decomposition and self de-coking over gadolinia-doped ceria supported Ni catalysts, Chem. Eng. J. 132 (2007) 97–103.